Clinical and Translational Radiation Oncology 26 (2021) 8–14

Contents lists available at ScienceDirect

Clinical and Translational Radiation Oncology

journal homepage: www.elsevier.com/locate/ctro

Original Research Article

The use of tumour markers in oesophageal cancer to quantify setup errors and baseline shifts during treatment

Melissa Thomas [a,b,*], Robin De Roover [a,b], Schalk van der Merwe [c], Maarten Lambrecht [a,b], Gilles Defraene [a], Karin Haustermans [a,b]

[a] KU Leuven – University of Leuven, Department of Oncology – Laboratory of Experimental Radiotherapy, Leuven, Belgium
[b] University Hospitals Leuven, Department of Radiation Oncology, Leuven, Belgium
[c] University Hospitals Leuven, Department of Gastroenterology and Hepatology, Leuven, Belgium

ARTICLE INFO

Article history:
Received 15 July 2020
Revised 1 November 2020
Accepted 1 November 2020
Available online 5 November 2020

Keywords:
Esophageal cancer
Fiducial gold markers
Inter-fractional motion
Intra-fractional baseline shifts
Radiotherapy treatment margins
Matching strategies

ABSTRACT

Purpose: To prospectively evaluate the feasibility of solid gold marker placement in oesophageal cancer patients and to quantify inter-fractional and intra-fractional (baseline shift) marker motion during radiation treatment. Radiotherapy target margins and matching strategies were investigated.
Materials/methods: Thirty-four markers were implanted by echo-endoscopy in 10 patients. Patients received a planning 4D CT, daily pre-treatment cone-beam CT (CBCT) and a post-treatment CBCT for at least five fractions. For fractions with both pre- and post-treatment CBCT, marker displacement between planning CT and pre-treatment CBCT (inter-fractional) and between pre-treatment and post-treatment CBCT (intra-fractional; only for fractions without rotational treatment couch correction) were calculated in left–right (LR), cranio-caudal (CC) and anterior-posterior (AP) direction after bony-anatomy and soft-tissue matching. Systematic/random setup errors were estimated; treatment margins were calculated.
Results: No serious adverse events occurred. Twenty-three (67.6%) markers were visible during radiotherapy (n = 3 middle oesophagus, n = 16 distal oesophagus, n = 4 proximal stomach). Margins for inter-fractional displacement after bony-anatomy match depended on the localisation of the primary tumour and were 11.2 mm (LR), 16.4 mm (CC) and 8.2 mm (AP) for distal markers. Soft-tissue matching reduced the CC margin for these markers (16.4 mm to 10.5 mm). The mean intra-fractional shift of 12 distal markers was 0.4 mm (LR), 2.3 mm (CC) and 0.7 mm (AP). Inclusion of this shift resulted in treatment margins for distal markers of 12.8 mm (LR), 17.3 mm (CC) and 10.4 mm (AP) after bony-anatomy matching and 12.4 mm (LR), 11.4 mm (CC) and 9.7 mm (AP) after soft-tissue matching.
Conclusion: This study demonstrated that the implantation of gold markers was safe, albeit less stable compared to other marker types. Inter-fractional motion was largest cranio-caudally for markers in the distal oesophagus, which was reduced after soft-tissue compared to bony-anatomy matching. The impact of intra-fractional baseline shifts on margin calculation was rather small.

1. Introduction

Oesophageal cancer is currently the seventh most common cancer worldwide and the sixth leading cause of cancer-related mortality [1]. For locoregionally advanced stages, neoadjuvant chemoradiation (nCRT) followed by surgery is currently the standard of care [2,3]. While this multimodality approach has demonstrated an overall survival benefit, the combination of radiotherapy and chemotherapy followed by surgery is associated with considerable morbidity and mortality [4,5]. In the literature, several studies revealed a correlation between the radiation dose to organs at

Abbreviations: 2D, two-dimensional; 3D, three-dimensional; 4D, four-dimensional; AP, anterior-posterior; CBCT, cone-beam computed tomography; CC, cranio-caudal; CT, computed tomography; CTV, clinical target volume; CTVtotal, total clinical target volume; DoF, degree-of-freedom; EUS, endoscopic ultrasound; FDG-PET/CT, fluorodeoxyglucose positron emission tomography with integrated computed tomography; GM, grand mean; GTV, gross tumour volume; iCTV, internal clinical target volume; IMRT, intensity modulated radiation therapy; kV, kilovoltage; LR, left-right; MRI, magnetic resonance imaging; nCRT, neoadjuvant chemoradiation; OAR, organ at risk; PTV, planning target volume.

* Corresponding author at: KU Leuven – University of Leuven, Department of Oncology – Laboratory of Experimental Radiotherapy, Leuven, Belgium.
E-mail address: melissa.thomas@uzleuven.be (M. Thomas).

https://doi.org/10.1016/j.ctro.2020.11.001

risk (OAR) and the incidence of complications [6–9]. The implementation of modern radiation delivery techniques, such as intensity modulated radiation therapy (IMRT) and proton therapy, allows to better sculpt the dose to the target volume and to reduce the dose to the OAR [10–14]. Uncertainties in tumour delineation and in inter- and intra-fractional position variation, however, lead to substantial irradiated volumes. This as a result of the use of large treatment margins or a robust optimisation strategy to compensate for these uncertainties during radiotherapy, leading to higher doses to OAR [15,16].

Nowadays, pre-treatment target position verification is routinely performed using two-dimensional (2D) kilovoltage (kV) x-ray imaging or cone-beam computed tomography (CBCT) [17–19]. Based on these images, bony anatomy or soft tissue is matched with its position on the planning computed tomography (CT) to correct for inter-fractional anatomical variations. However, the actual tumour position can have a residual displacement with respect to its planned position after performing this matching [20,21]. Several studies have investigated the mobility of oesophageal tumours. The inter-fractional displacement has been quantified based on repeated CBCT or (four-dimensional (4D)) CT during the radiotherapy treatment [17,20,22]. Also fiducial markers, inserted inside the tumour, have been used to study the inter-fractional shift by the use of kV images or CBCT [19,23–25]. In most studies, the motion was largest cranio-caudally and for tumours in the distal oesophagus [19,23,24]. The intra-fractional motion has been studied by the use of CT on rails or cine-magnetic resonance imaging (MRI) before and during radiotherapy [20,21,26,27]. One study investigated the intra-fractional tumour motion, defined as the combined cardiac and respiratory motion, by estimating the three-dimensional (3D) trajectory of intra-tumoural fiducial markers during the CBCT acquisition [24]. Implanted markers were also used to analyse the respiratory motion in a planning 4D CT before treatment or on reconstructed 4D CBCT [28,29].

Many of these studies used intra-tumoural fiducial markers as these are a highly visible surrogate for the tumour. However, fiducial markers are implanted by endoscopy, an invasive procedure which can involve complications [30]. Moreover, markers can migrate and the visibility during radiotherapy treatment is not always guaranteed [24,30]. Furthermore, the role of intra-tumoural fiducial markers in pre-treatment target position verification is not yet clear. One study demonstrated that an automatic marker-based registration was not reliable in most of the CBCT scans and that a manual marker-based registration was very time-consuming and challenging due to tumour deformation [30].

The aim of this study was to prospectively evaluate the feasibility of solid gold marker placement in 10 oesophageal cancer patients. The inter- and intra-fractional marker motion during the radiation treatment was quantified. Radiotherapy treatment margins and matching strategies were investigated.

2. Materials/methods

2.1. Patients and treatment

Ten patients with an adenocarcinoma of the oesophagus scheduled for nCRT between May 2018 and September 2019 were included in this trial. The study was approved by the Institutional Ethical Review Board of the University Hospitals of Leuven (S60601).

Pre-treatment evaluations included a complete medical history and physical examination; complete blood count and biochemical survey; fluorodeoxyglucose (FDG) positron emission tomography (PET) with integrated CT (FDG-PET/CT) scan; oesophagogastroduodenoscopy with biopsy; and an endoscopic ultrasound (EUS) of the oesophagus.

Radiotherapy was delivered in fractions of 1.8 Gy to a total dose of 45.0 Gy using IMRT, concomitant with carboplatin-paclitaxel. The gross tumour volume (GTV) was delineated with the use of all available information (e.g. endoscopy, EUS, diagnostic (FDG-PET/)CT, fiducial markers). The GTV was expanded with an isotropic margin of 3.0 cm cranio-caudally and 1.0 cm radially to the clinical target volume (CTV) of the primary tumour. The CTV of the lymph nodes included the involved lymph nodes with a margin of 0.5 cm, the involved lymph node stations and the lymph node stations along the CTV of the primary tumour. The CTV of the primary tumour and lymph nodes formed the total CTV (CTVtotal). The internal CTV (iCTV) was defined as the sum of the CTVtotal in all phases of the planning 4D CT scan to account for respiratory motion. An isotropic planning target volume (PTV) margin of 0.7 cm was added to the iCTV.

2.2. Marker implantation and data acquisition

All patients underwent an EUS-guided implantation of at least three markers in the submucosal layer at the upper and lower border and in the centre of the primary tumour. A preloaded, 22-gauge EchoTip Ultra Fiducial Needle (Cook Medical, Limerick, Ireland) was used. Each needle contained four solid gold fiducial markers, measuring 5.0 mm in length by 0.43 to 0.6 mm in diameter. The markers were classified in anatomical subgroups based on their position according to the Union for International Cancer Control (UICC) TNM staging system (eighth edition) [31]. A serious adverse event was defined as an event that results in death, or is life-threatening, or results in persistent or significant disability/incapacity, or requires or prolongs inpatient hospitalisation, or is considered an important medical event (e.g. mediastinitis).

Patients were positioned supine (Posirest and knee support) and received a phase-sorted planning 4D CT with a SOMATOM Sensation Open (3/10 patients) or a SOMATOM Drive (7/10 patients) CT scanner (Siemens, Erlangen, Germany) within seven days after marker placement. All CT images were reconstructed at 3.0 mm slice thickness and no metal artefact reduction was used. The average CT was used for delineation and treatment planning. Daily kV CBCT scans were acquired for pre-treatment position verification using the on-board imager of a TrueBeam (3/10 patients) or Halcyon (7/10 patients) linear accelerator (Varian Medical Systems, Palo Alto, CA, USA). The standard thorax scanning protocol was used on both linacs and the CBCT images were reconstructed at 2.0 mm slice thickness. A six degree-of-freedom (DoF) couch correction was performed using the PerfectPitch couch for patients treated on the TrueBeam linac whereas a three DoF couch correction was performed for patients treated on the Halcyon linac. In addition, a post-treatment CBCT scan was acquired immediately after treatment delivery for at least five fractions to investigate the intra-fraction mobility of the tumour. The time between the pre-treatment and post-treatment CBCT scans was recorded.

2.3. Technical feasibility of marker placement

The technical feasibility of marker implantation was defined as the ability to successfully implant three or more markers. The visibility of the markers was monitored throughout the entire radiotherapy treatment course. Both the time between marker implantation and the planning CT scan and the time between marker implantation and the start of the radiotherapy treatment were recorded.

2.4. Inter-fractional marker displacement

For each patient, individual markers were manually contoured on the average planning CT image and on the CBCT images of all the fractions that had both a pre-treatment and post-treatment CBCT scan. The position of each marker was then defined as the centre of mass of the marker segmentation. To investigate the influence of different setup strategies, each pre-treatment CBCT scan was matched with the planning CT on both bony-anatomy and on soft-tissue using an automatic registration in Image Registration (Varian Medical Systems) followed by a visual inspection of the alignment of the scans. For bony-anatomy match, a clipbox (i.e. region of interest) was placed partially around the thoracic vertebrae along the iCTV. Soft-tissue matching was performed using a clipbox encompassing the iCTV with an isotropic margin of approximately 1.0 cm. Subsequently, the individual marker displacement between each pre-treatment CBCT and the reference position on the planning CT was calculated in the left–right (LR), craniocaudal (CC) and anterior-posterior (AP) direction for both matching strategies. The mean and standard deviation of the inter-fractional marker displacements were calculated over all the analysed fractions of each marker. The grand mean (GM) was calculated together with the standard deviation of the mean displacement of each marker as the latter is an estimate of the systematic error (Σ). The random error (σ) was estimated by the root mean square of the standard deviation of the displacements of each marker.

The margin required to compensate for the inter-fractional position variation of oesophageal tumours to deliver at least 95% dose to the CTV in 90% of the patients was calculated using the formula by Van Herk et al. [32]:

$$M = 2,5 \times \sum + 1,64 \times \left[\sqrt{\sigma^2 + \sigma_p^2} - \sigma_p\right]$$

Margins were calculated for all studied markers combined and for each of the anatomical subgroup of markers separately. The penumbra width characterization (σ_p) was set to 3.0 mm.

2.5. Intra-fractional marker displacement

The marker displacement between the post-treatment and pre-treatment CBCT image of the analysed fractions was calculated for each marker to investigate the occurrence of intra-fractional shifts during treatment delivery. The treatment couch shift applied between setup CBCT and treatment delivery was subtracted from the observed marker displacement. Fractions with a rotational treatment couch correction were excluded from the analysis as it was not possible to subtract the couch correction from the observed marker displacement. The impact of the intra-fractional mobility on the treatment margin was estimated by including the systematic error ($\sum_{intra}$) and the random error (σ_{intra}) of the intrafraction marker displacements through $\sum = \sqrt{\sum_{inter}^2 + \sum_{intra}^2}$ and $\sigma = \sqrt{\sigma_{inter}^2 + \sigma_{intra}^2}$ [33].

2.6. Statistical analysis

All statistical analyses were performed using Matlab R2017b (Mathworks, Natick, MA, USA).

3. Results

Patient characteristics are presented in Table A.1. All patients were men. One patient had a supraclavicular pathological lymph node and received 41.4 Gy due to the large irradiated volume and the tolerance of the OAR, especially the lungs. One patient had seven post-treatment CBCT scans instead of five due to miscommunication.

Fiducial marker implantation was successful in 70.0% of the patients (i.e. three or more markers implanted in seven patients) (Table A.1). A total of 34 markers were placed in 10 patients, three in the middle oesophagus, 24 in the distal oesophagus and seven in the proximal stomach. No serious adverse events occurred. The median time to the planning CT scan after marker placement was 2,5 days (range 0–7 days). The median time between implantation and the first CBCT scan at the start of radiotherapy was 14 days (range 12–19 days). Six markers detached before the planning 4D CT scan, five markers in the distal oesophagus and one in the proximal stomach. Five markers detached after the planning CT scan before the start of radiotherapy, three in the distal oesophagus and two in the proximal stomach. So respectively 28 (82.4%) and 23 (67.6%) markers were visible on the planning CT scan and the first CBCT scan. No markers were lost during treatment.

The mean shift of the tumour relative to bony-anatomy was largest in the CC direction for markers in the distal oesophagus (GM of −2.4 mm) (Table 1). For markers in the proximal stomach, the AP motion was dominant (GM of 6.4 mm). The maximum shift of all studied marker displacements for all patients after bony-anatomy match was 12.5 mm, 14.0 mm and 20.5 mm in LR, CC and AP direction respectively (Fig. 1). The outliers of shifts of more than 15.0 mm were all caused by markers in the proximal stomach. Two of them showed an increase in the AP direction up to 20.5 mm by the end of treatment (Fig. 1). The estimated systematic and random errors after bony-anatomy match are shown in Table 1. The margins for the inter-fractional displacement depended on the localisation of the primary tumour in the oesophagus (Table 1) (Fig. 2). Anisotropic margins were obtained, respectively 11.2 mm, 16.4 mm and 8.2 mm in the LR, CC and AP direction for markers in the distal oesophagus. With soft-tissue matching, the systematic shift of the inter-fractional displacement in the CC direction decreased for markers in the distal oesophagus (GM of 0.3 mm) (Table 1). The maximum shift of all studied marker displacements for all patients after soft-tissue matching was 12.9 mm, 17.4 mm and 21.4 mm in the LR, CC and AP direction respectively (Fig. 1). The estimated systematic and random errors after soft-tissue matching are shown in Table 1. Soft-tissue matching reduced the margin in the CC direction for markers in the distal oesophagus from 16.4 mm to 10.5 mm. This reduction was less pronounced in the LR and AP direction.

Median time between the CBCT before and after each fraction was 5 min 57 s (3 min 18 s–20 min 06 s). The mean intra-fractional shift of the 12 markers included in the analyses for calculation of the intra-fractional marker displacement (all distal markers) was 0.4 mm, 2.3 mm and 0.7 mm in LR, CC and AP direction respectively. There was no time trend in the marker shifts over the treatment course (Fig. 3). Inclusion of the intra-fraction shift resulted in treatment margins for distal markers of 12.8 mm (LR), 17.3 mm (CC) and 10.4 mm (AP) after bony-anatomy matching and 12.4 mm (LR), 11.4 mm (CC) and 9.7 mm (AP) after soft-tissue matching (Table 1).

4. Discussion

In this study, 34 solid gold fiducial markers were implanted in 10 patients with oesophageal cancer. Twenty-three markers could be used to quantify the inter- and intra-fractional motion and its implications on margins after bony-anatomy and soft-tissue match.

The technical feasibility of marker implantation was defined as the ability to implant three or more markers, which was successful in seven of 10 patients. In three patients, this was not possible due

Table 1
Inter-fraction and intra-fraction shift for all markers and marker subgroups after bony-anatomy and soft-tissue match.

	Bony-anatomy match (mm)			Soft-tissue match (mm)		
	LR	CC	AP	LR	CC	AP
All markers (n = 23)						
GM	−0.4	−2.7	0.5	0.2	1.1	0.6
$\sum_{inter}$	3.5	4.9	4.4	3.5	3.7	4.2
σ_{inter}	2.7	3.1	3.0	2.5	3.6	3.4
$\sum_{intra}$[$]	1.6	1.3	2.5	1.6	1.3	2.5
σ_{intra}[$]	2.9	2.2	3.4	2.9	2.2	3.4
$Margin_{inter}$	10.4	14.5	13.1	10.1	12.1	13.0
$Margin_{inter+intra}$	12.8	15.7	16.7	12.5	13.4	16.6
Middle oesophagus (n = 3)						
GM	1.1	−1.5	−0.5	2.0	0.1	0.6
$\sum_{inter}$	0.6	1.5	2.0	0.9	2.5	1.7
σ_{inter}	1.4	1.5	0.8	1.4	1.9	0.9
$Margin_{inter}$	2.0	4.3	5.1	2.9	7.2	4.5
Distal oesophagus (n = 16)						
GM	−0.3	−2.4	−0.8	0.2	0.3	−0.8
$\sum_{inter}$	3.9	5.8	2.9	3.8	3.4	2.6
σ_{inter}	2.5	2.9	2.0	2.2	3.0	2.0
$\sum_{intra}$[$]	1.6	1.3	2.5	1.6	1.3	2.5
σ_{intra}[$]	2.9	2.2	3.4	2.9	2.2	3.4
$Margin_{inter}$	11.2	16.4	8.2	10.8	10.5	7.5
$Margin_{inter+intra}$	12.8	17.3	10.4	12.4	11.4	9.7
Proximal stomach (n = 4)						
GM	−1.7	−4.7	6.4	−1.3	5.2	6.3
$\sum_{inter}$	3.0	1.6	6.6	2.6	3.7	6.3
σ_{inter}	3.9	4.4	5.8	3.7	6.0	7.1
$Margin_{inter}$	10.6	8.0	22.3	9.4	15.4	23.5

n = number, LR = left-right, CC = cranio-caudal; AP = anterior-posterior; GM = grand mean; $\sum$ = standard deviation of the systematic error; σ = root mean square of standard deviations of random errors; inter = inter-fraction; intra = intra-faction.
[$] Based on 12 distal markers.

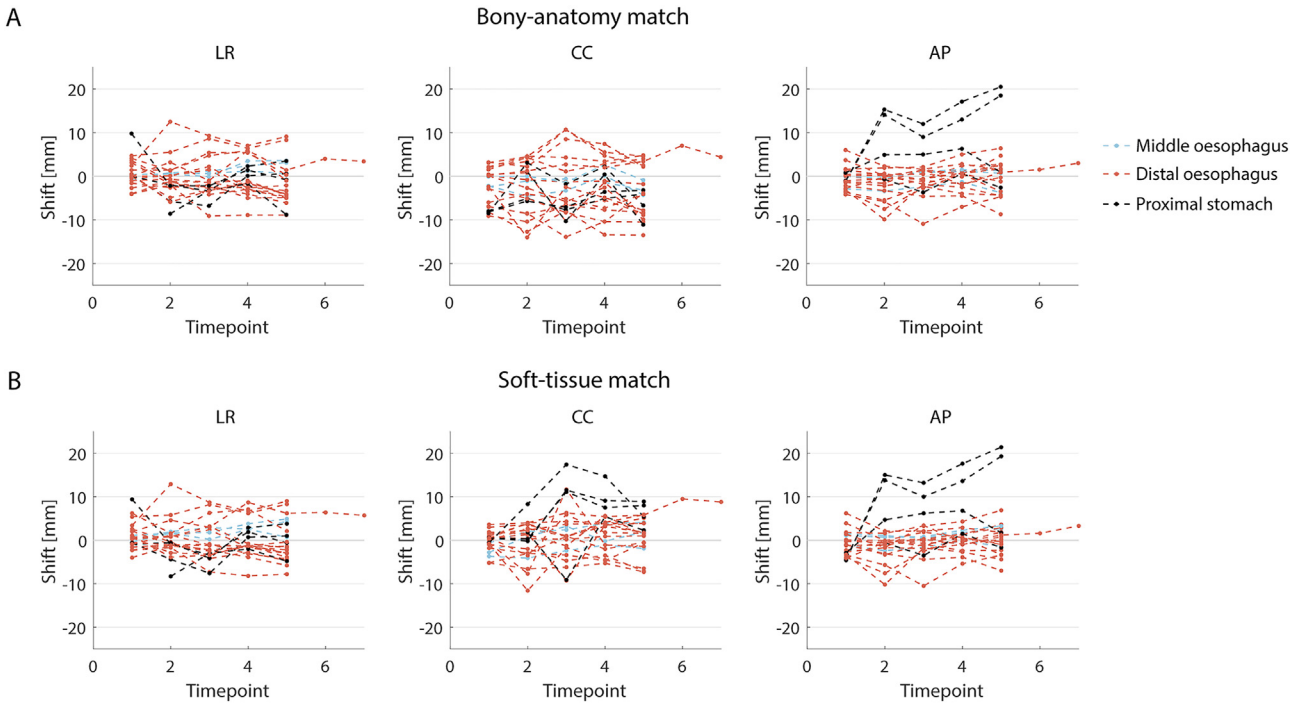

Fig. 1. Marker shift over the treatment course on the pre-treatment CBCTs after bony-anatomy and soft-tissue match. The time dependency of markers in the middle and distal oesophagus and in the proximal stomach are presented after bony-anatomy (A) and soft-tissue (B) match. Two markers in the proximal stomach showed an increase in the AP direction up to 20.5 mm and 21.4 mm after bony-anatomy and soft-tissue match respectively. LR = left-right; CC = cranio-caudal; AP = anterior-posterior.

to technical issues, e.g. accidental insertion of two markers in the same position which counted as one or loss of the marker during insertion. The marker implantation was safe, without the occurrence of serious adverse events. Of the 34 implanted markers, 82% (28 markers) were visible on the planning CT scan. This was lower compared to previous studies with solid gold markers

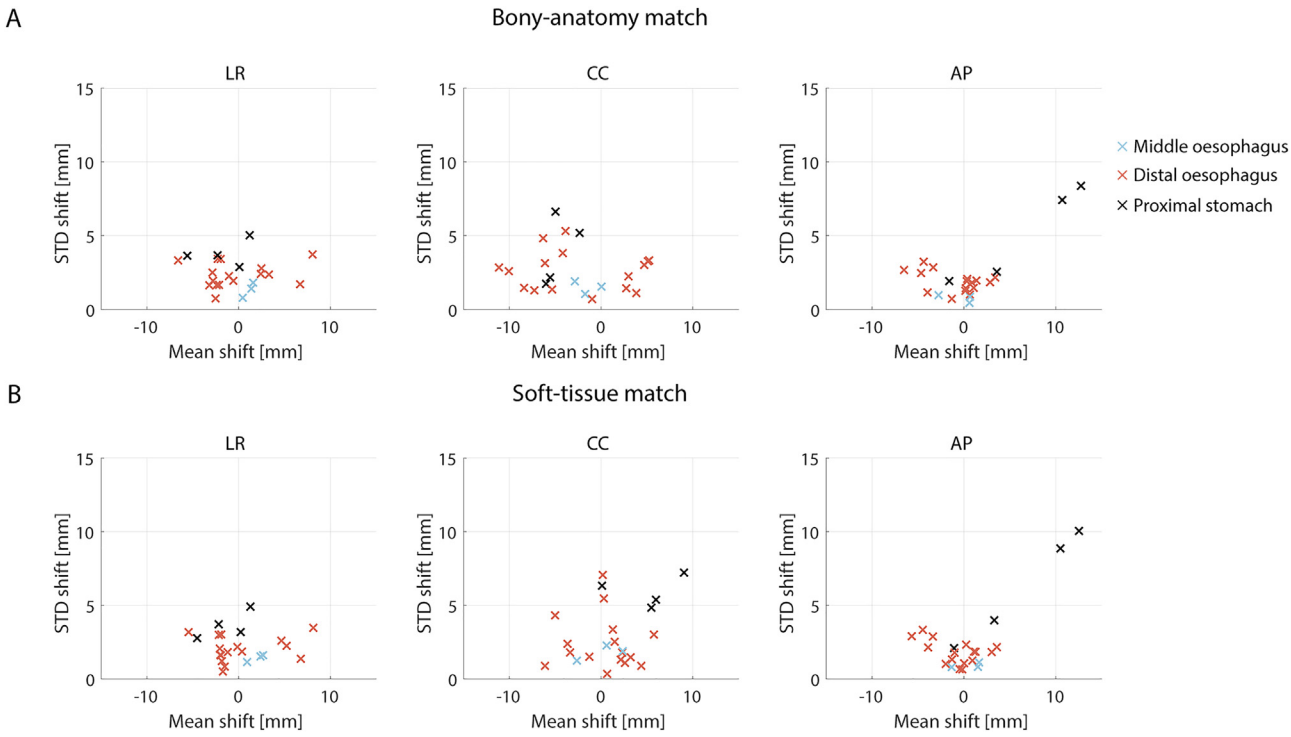

Fig. 2. Scatter plot of markers on the pre-treatment CBCTs based on bony-anatomy and soft-tissue match. Scatter plot of the mean (x-axis) against the standard deviation (y-axis) over the five fractions of markers in the middle and distal oesophagus and in the proximal stomach are presented after bony-anatomy (A) and soft-tissue (B) match. LR = left-right; CC = cranio-caudal; AP = anterior-posterior.

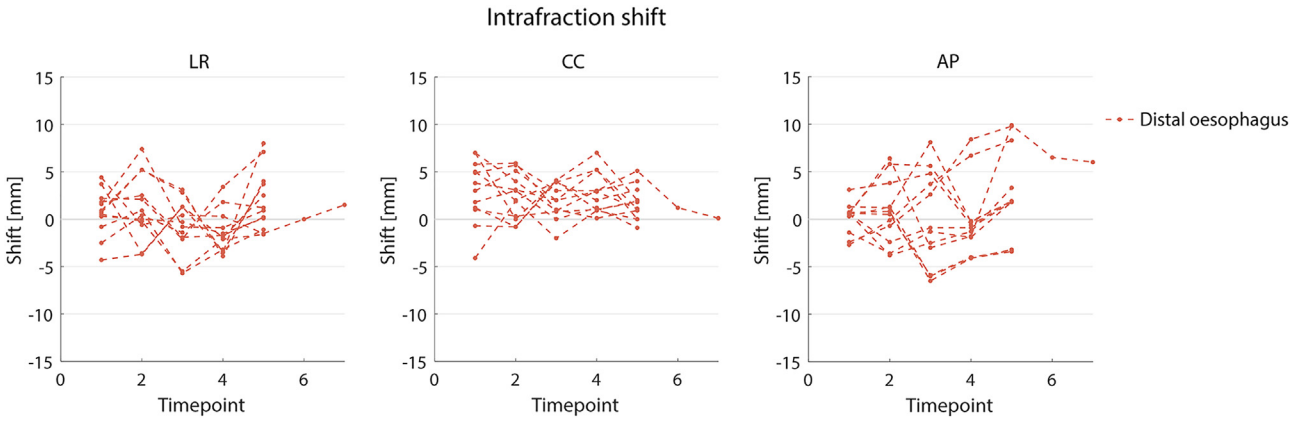

Fig. 3. The intra-fractional shift of the markers over the treatment course. The time dependency of the intra-fractional shift of the 12 distal markers is presented. There was no time trend in the marker shifts over the treatment course. LR = left-right; CC = cranio-caudal; AP = anterior-posterior.

(88%) [24,30]. In addition, 68% of the markers were visible during the treatment on the CBCT scans, which was higher than in the study of Machiels et al., but lower than in the study of Hoffman et al. (63% and 81% with gold markers respectively) [24,30]. Based on our results, the use of solid gold markers seems to be discouraging. Also in another study, the feasibility of implantation and visibility during treatment of these markers were inferior compared to other types, such as coil-shaped gold markers [30]. The latter were recently used in oesophageal cancer patients treated with proton therapy and previous studies reported no considerable dose perturbations with this marker type [25,34,35].

The inter-fractional motion after bony-anatomy match was larger in our study compared to those observed in previous studies [23,24]. However, similar to these studies, the systematic and random error for distal markers were less pronounced in the LR and AP direction, which may be explained by the close proximity of the vertebrae, the lungs and the heart that encompass the oesophagus. The more pronounced systematic error in the CC direction resulted in a larger and anisotropic margin cranio-caudally to compensate for inter-fractional motion. The large systematic and random errors in the AP direction for tumour markers in the proximal stomach could be attributed to daily variations in gastric filling. Consequently, a larger margin in the AP direction could be needed for tumours beneath the diaphragm, which was demonstrated previously [24]. However, it should be noted that our findings relate to only four markers in the proximal stomach. In our study, three markers in the middle oesophagus were visible during treatment, so the margins obtained for this anatomical subgroup are subject to uncertainties. The overall calculated margins were therefore dominated by the markers in the distal oesophagus.

Soft-tissue matching was performed retrospectively and reduced the margin in the CC direction for markers in the distal oesophagus, comparable with previous results [24]. A margin reduction was not seen for markers in the middle oesophagus or the proximal stomach, probably due to the low number of markers at this location.

To calculate the intra-fractional shift, we used the CBCT performed after treatment. Comparing the pre-treatment and post-treatment CBCT scan allowed to observe the baseline shifts that may occur during treatment delivery. This shift was largest in the CC direction (only markers in the distal oesophagus). The impact on the treatment margins however was small.

When calculating radiotherapy treatment margins, several issues have to be considered. By using intra-tumoural markers for margin calculation, we assume that the motion of the GTV is a surrogate for the CTV. Although, large treatment volumes are frequently used to encompass subclinical spread along the oesophagus (often 3.0 cm from GTV to CTV). The primary tumour can however easily be demarcated, whereas markers implantation is more challenging in normal oesophagus and upfront demarcation of the CTV by echo-endoscopy is not possible. Moreover, respiratory motion is partially incorporated in the CTV, as the PTV-margin is obtained by expansion of the iCTV in case of a planning 4D CT. Additionally, the calculation of margins is biased due to centre-specific uncertainties, such as patient setup uncertainties and inter-observer variability for matching.

A limitation of the study was the small sample size of 10 patients. In addition, our results are mainly applicable for tumours in the distal oesophagus, as most markers were implanted at this location and the calculation of the intra-fractional motion was based on distal markers only. A novelty of our study was the use of a post-treatment CBCT to calculate baseline shifts. The respiratory motion was not integrated. The inter-fractional and intra-fractional displacements were calculated from the center of mass position of the delineated markers. As such, the influence of respiratory motion on the analyses will be limited in case of a regular breathing motion as this would not affect the average position of the marker. The CBCT scans were verified for breathing motion related artefacts to exclude irregular breathing motion during CBCT acquisition. Additionally, in oesophageal cancer, respiratory motion can be mitigated through the use of an iCTV based on the motion observed on the planning 4D CT [36–38]. The inter-fractional variability of respiratory motion was investigated by Jin et al. by comparing a reconstructed 4D CBCT with the planning 4D CT [29]. They found that this motion on the planning 4D CT is sufficient for predicting the respiration-induced oesophageal tumour motion during treatment. Lastly, there was a difference in slice thickness of the planning CT and the CBCTs (3.0 mm and 2.0 mm). This, together with marker artefacts on the imaging, could lead to an uncertainty on marker delineation and a small overestimation of the margins.

In conclusion, this study demonstrated that the implantation of solid gold markers was safe but showed less stability compared to those reported for other marker types, such as coil-shaped markers. The inter-fractional motion was largest cranio-caudally for markers in the distal oesophagus, which was reduced after soft-tissue matching compared to bony-anatomy matching. The impact of intra-fractional motion on the margins was rather small.

Declaration of Competing Interest

The authors declare that they have no known competing financial interests or personal relationships that could have appeared to influence the work reported in this paper.

Acknowledgements

Melissa Thomas, Robin De Roover and Gilles Defraene were supported by Kom op tegen Kanker (Stand up to Cancer), the Flemish cancer society. Karin Haustermans was a senior clinical investigator at the Research Foundation Flanders (FWO).

Appendix A. Supplementary data

Supplementary data to this article can be found online at https://doi.org/10.1016/j.ctro.2020.11.001.

References

[1] Bray F, Ferlay J, Soerjomataram I, Siegel RL, Torre LA, Jemal A. Global Cancer Statistics 2018: GLOBOCAN estimates of incidence and mortality worldwide for 36 Cancers in 185 countries. CA Cancer J Clin 2018;68:394–424. https://doi.org/10.3322/caac.21492.

[2] Lordick F, Mariette C, Haustermans K, Obermannová R, Arnold D. Oesophageal cancer: ESMO Clinical Practice Guidelines for diagnosis, treatment and follow-up. Ann Oncol 2016;27:v50–7. https://doi.org/10.1093/ANNONC/MDW329.

[3] National Comprehensive Cancer Network. Clinical Practice Guidelines in Oncology, NCCN Guidelines Version 2.2020: Esophageal and Esophagogastric Junction Cancers 2020.

[4] Bosch DJ, Muijs CT, Mul VEM, Beukema JC, Hospers GAP, Burgerhof JGM, et al. Impact of neoadjuvant chemoradiotherapy on postoperative course after curative-intent transthoracic esophagectomy in esophageal cancer patients. Ann Surg Oncol 2014;21:605–11. https://doi.org/10.1245/s10434-013-3316-8.

[5] Reynolds JV, Ravi N, Hollywood D, Kennedy MJ, Rowley S, Ryan A, et al. Neoadjuvant chemoradiation may increase the risk of respiratory complications and sepsis after transthoracic esophagectomy. J Thorac Cardiovasc Surg 2006;132:549–55. https://doi.org/10.1016/j.jtcvs.2006.05.015.

[6] Lee HK, Vaporciyan AA, Cox JD, Tucker SL, Putnam JB, Ajani JA, et al. Postoperative pulmonary complications after preoperative chemoradiation for esophageal carcinoma: correlation with pulmonary dose–volume histogram parameters. Int J Radiat Oncol Biol Phys 2003;57:1317–22. https://doi.org/10.1016/S0360-3016(03)01373-7.

[7] Wang SL, Liao Z, Vaporciyan AA, Tucker SL, Liu H, Wei X, et al. Investigation of clinical and dosimetric factors associated with postoperative pulmonary complications in esophageal cancer patients treated with concurrent chemoradiotherapy followed by surgery. Int J Radiat Oncol Biol Phys 2006;64:692–9. https://doi.org/10.1016/j.ijrobp.2005.08.002.

[8] Tucker SL, Liu HH, Wang S, Wei X, Liao Z, Komaki R, et al. Dose-volume modeling of the risk of postoperative pulmonary complications among esophageal cancer patients treated with concurrent chemoradiotherapy followed by surgery. Int J Radiat Oncol Biol Phys 2006;66:754–61. https://doi.org/10.1016/j.ijrobp.2006.06.002.

[9] Hatakenaka M, Yonezawa M, Nonoshita T, Nakamura K, Yabuuchi H, Shioyama Y, et al. Acute cardiac impairment associated with concurrent chemoradiotherapy for esophageal cancer: magnetic resonance evaluation. Int J Radiat Oncol Biol Phys 2012;83:e67–73. https://doi.org/10.1016/j.ijrobp.2011.12.018.

[10] Chandra A, Guerrero TM, Liu HH, Tucker SL, Liao Z, Wang X, et al. Feasibility of using intensity-modulated radiotherapy to improve lung sparing in treatment planning for distal esophageal cancer. Radiother Oncol 2005;77:247–53. https://doi.org/10.1016/j.radonc.2005.10.017.

[11] Kole TP, Osarhieme A, Kwah J, Yorke ED, Goodman KA. Comparison of heart and coronary artery doses associated with intensity-modulated radiotherapy versus three-dimensional conformal radiotherapy for distal esophageal cancer. Int J Radiat Oncol Biol Phys 2012;83:1580–6. https://doi.org/10.1016/j.ijrobp.2011.10.053.

[12] Welsh J, Gomez D, Palmer MB, Riley BA, Mayankkumar AV, Komaki R, et al. Intensity-modulated proton therapy further reduces normal tissue exposure during definitive therapy for locally advanced distal esophageal tumors: a dosimetric study. Int J Radiat Oncol Biol Phys 2011;81:1336–42. https://doi.org/10.1016/j.ijrobp.2010.07.2001.

[13] Shiraishi Y, Xu C, Yang J, Komaki R, Lin SH. Dosimetric comparison to the heart and cardiac substructure in a large cohort of esophageal cancer patients treated with proton beam therapy or intensity-modulated radiation therapy. Radiother Oncol 2017;125:48–54. https://doi.org/10.1016/j.radonc.2017.07.034.

[14] Wang J, Palmer M, Bilton SD, Vu KN, Greer S, Frame R, et al. Comparing proton beam to intensity modulated radiation therapy planning in esophageal cancer. Int J Part Ther 2015;1:866–77. https://doi.org/10.14338/IJPT-14-00018.1.

[15] van Herk M. Errors and margins in radiotherapy. Semin Radiat Oncol 2004;14:52–64. https://doi.org/10.1053/j.semradonc.2003.10.003.

[16] Paganetti H. Range uncertainties in proton therapy and the role of Monte Carlo simulations. Phys Med Biol 2012;57:R99–R117. https://doi.org/10.1088/0031-9155/57/11/R99.

[17] Yamashita H, Haga A, Hayakawa Y, Okuma K, Yoda K, Okano Y, et al. Patient setup error and day-to-day esophageal motion error analyzed by cone-beam computed tomography in radiation therapy. Acta Oncol (Madr) 2010;49:485–90. https://doi.org/10.3109/02841861003652574.
[18] Hawkins MA, Aitken A, Hansen VN, McNair HA, Tait DM. Set-up errors in radiotherapy for oesophageal cancers – is electronic portal imaging or conebeam more accurate?. Radiother Oncol 2011;98:249–54. https://doi.org/10.1016/j.radonc.2010.11.002.
[19] Fukada J, Hanada T, Kawaguchi O, Ohashi T, Takeuchi H, Kitagawa Y, et al. Detection of esophageal fiducial marker displacement during radiation therapy with a 2-dimensional on-board imager: analysis of internal margin for esophageal cancer. Int J Radiat Oncol Biol Phys 2013;85:991–8. https://doi.org/10.1016/j.ijrobp.2012.07.2358.
[20] Cohen RJ, Paskalev K, Litwin S, Price Jr R, Feigenberg SJ, Konski A. Esophageal motion during radiotherapy: quantification and margin implications. Dis Esophagus 2010;23:473–9. https://doi.org/10.1111/j.1442-2050.2009.01037.x.
[21] Heethuis SE, Borggreve AS, Goense L, van Rossum PSN, Mook S, van Hillegersberg R, et al. Quantification of variations in intra-fraction motion of esophageal tumors over the course of neoadjuvant chemoradiotherapy based on cine-MRI. Phys Med Biol 2018;63:. https://doi.org/10.1088/1361-6560/aacfb5145019.
[22] Wang J, Lin SH, Dong L, Balter P, Mohan R, Komaki R, et al. Quantifying the interfractional displacement of the gastroesophageal junction during radiation therapy for esophageal cancer. Int J Radiat Oncol Biol Phys 2012;83:e273–80. https://doi.org/10.1016/j.ijrobp.2011.12.048.
[23] Jin P, van der Horst A, de Jong R, van Hooft JE, Kamphuis M, van Wieringen N, et al. Marker-based quantification of interfractional tumor position variation and the use of markers for setup verification in radiation therapy for esophageal cancer. Radiother Oncol 2015;117:412–8. https://doi.org/10.1016/j.radonc.2015.10.005.
[24] Hoffmann L, Poulsen PR, Ravkilde T, Bertholet J, Kruhlikava I, Helbo BL, et al. Setup strategies and uncertainties in esophageal radiotherapy based on detailed intra- and interfractional tumor motion mapping. Radiother Oncol 2019;136:161–8. https://doi.org/10.1016/j.radonc.2019.04.014.
[25] Apolle R, Brückner S, Frosch S, Rehm M, Thiele J, Valentini C, et al. Utility of fiducial markers for target positioning in proton radiotherapy of oesophageal carcinoma. Radiother Oncol 2019;133:28–34. https://doi.org/10.1016/j.radonc.2018.12.016.
[26] Lever FM, Lips IM, Crijns SPM, Reerink O, Van Lier ALHMW, Moerland MA, et al. Quantification of esophageal tumor motion on cine-magnetic resonance imaging. Int J Radiat Oncol Biol Phys 2014;88:419–24.. https://doi.org/10.1016/j.ijrobp.2013.10.036.
[27] Zhou H-Y, Zhang J-G, Li R, Zhang X-M, Chen T-W, Liu N, et al. Tumour motion of oesophageal squamous cell carcinoma evaluated by cine MRI: associated with tumour location. Clin Radiol 2018;73:676.e1–7. https://doi.org/10.1016/j.crad.2018.02.006.
[28] Yamashita H, Kida S, Sakumi A, Haga A, Ito S, Onoe T, et al. Four-dimensional measurement of the displacement of internal fiducial markers during 320-multislice computed tomography scanning of thoracic esophageal cancer. Int J Radiat Oncol Biol Phys 2011;79:588–95. https://doi.org/10.1016/j.ijrobp.2010.03.045.
[29] Jin P, Hulshof MCCM, van Wieringen N, Bel A, Alderliesten T. Interfractional variability of respiration-induced esophageal tumor motion quantified using fiducial markers and four-dimensional cone-beam computed tomography. Radiother Oncol 2017. https://doi.org/10.1016/j.radonc.2017.05.015.
[30] Machiels M, van Hooft J, Jin P, van Berge Henegouwen MI, van Laarhoven HM, Alderliesten T, et al. Endoscopy/EUS-guided fiducial marker placement in patients with esophageal cancer: a comparative analysis of 3 types of markers. Gastrointest Endosc 2015;82:641–9. https://doi.org/10.1016/j.gie.2015.03.1972.
[31] Brierley JD, Gospodarowicz MK, Wittekind C. Oesophagus (ICD-O-3 C15) – including oesophagogastric junction (C16). UICC TNM classification of malignant tumours. 8th ed. Wiley-Blackwell; 2017.
[32] van Herk M, Remeijer P, Rasch C, Lebesque JV. The probability of correct target dosage: dose-population histograms for deriving treatment margins in radiotherapy. Int J Radiat Oncol Biol Phys 2000;47:1121–35. https://doi.org/10.1016/S0360-3016(00)00518-6.
[33] Yan D, Lockman D, Martinez A, Wong J, Brabbins D, Vicini F, et al. Computed tomography guided management of interfractional patient variation. Semin Radiat Oncol 2005;15:168–79. https://doi.org/10.1016/j.semradonc.2005.01.007.
[34] Habermehl D, Henkner K, Ecker S, Jäkel O, Debus J, Combs SE. Evaluation of different fiducial markers for image-guided radiotherapy and particle therapy. J Radiat Res 2013;54:61–8. https://doi.org/10.1093/jrr/rrt071.
[35] Giebeler A, Fontenot J, Balter P, Ciangaru G, Zhu R, Newhauser W. Dose perturbations from implanted helical gold markers in proton therapy of prostate cancer. J Appl Clin Med Phys 2009;10:2875.
[36] Zhao K, Liao Z, Bucci MK, Komaki R, Cox JD, Yu ZH, et al. Evaluation of respiratory-induced target motion for esophageal tumors at the gastroesophageal junction. Radiother Oncol 2007;84:283–9. https://doi.org/10.1016/j.radonc.2007.07.008.
[37] Zhang X, Zhao K, Guerrero TM, Mcguire SE, Yaremko B, Komaki R, et al. Four-dimensional computed tomography-based treatment planning for intensity-modulated radiation therapy and proton therapy for distal esophageal cancer. Int J Radiat Oncol Biol Phys 2008;72:278–87. https://doi.org/10.1016/j.ijrobp.2008.05.014.
[38] Patel AA, Wolfgang JA, Niemierko A, Hong TS, Yock T, Choi NC. Implications of respiratory motion as measured by four-dimensional computed tomography for radiation treatment planning of esophageal cancer. Int J Radiat Oncol Biol Phys 2009;74:290–6. https://doi.org/10.1016/j.ijrobp.2008.12.060.